



WFC3 Instrument Science Report 2008-24

# WFC3 TV3 Testing: IR Channel Thermal Background Signal

B. Hilbert  
December 16, 2008

---

## ABSTRACT

*Using data taken during thermal vacuum 3 (TV3) testing, we have measured the magnitude and stability of the dark current plus thermal background signal present in WFC3's IR channel. We find that the IR channel with the flight detector (IR4) meets the Contract End Item (CEI) specifications for total background signal and background stability. Additionally, the background levels presented here should be interpreted as upper limits, due to persistence effects from a previous test.*

---

## Introduction

During TV3 testing in the spring of 2008, data were taken using WFC3's IR channel to measure the amount of thermal background flux seen by the detector through all filters. This test was performed during TV1 and TV2, using backup focal plane arrays (FPAs). The TV3 iteration of this test repeated that in TV2, with an eye toward comparing the higher-QE flight FPA (FPA165) versus the backup FPA (FPA129) used in TV2.

## Data

The IR01S08 Science Mission Specification (SMS) was run only once during TV3 testing. This SMS collected one data ramp each in most of the IR channel filters, interspersed with dark current ramps. Details of the data are listed in Table 1. The total duration of the test was roughly 2.5 hours, limiting our analysis of the thermal

background to this timescale. The dark current ramps in this test were taken in the standard fashion, with the aluminum blank inserted into the optical path. The background ramps, with the filters in place, were taken with the detector staring at the unilluminated IR optical path of WFC3 and the warm optics of the optical stimulus (referred to as “CASTLE”). All CASTLE light sources were shuttered or turned off.

<b>Filter</b>	<b>Sample Sequence</b>	<b>Reads per Ramp</b>	<b>Exp Time (sec)</b>
F098M	SPARS100	4	202.9
F105W	SPARS100	4	202.9
F110W	SPARS100	4	202.9
F125W	SPARS100	4	202.9
F126N	SPARS100	4	202.9
F127M	SPARS100	4	202.9
F128N	SPARS100	4	202.9
F130N	SPARS100	4	202.9
F132N	SPARS100	4	202.9
F139M	SPARS100	4	202.9
F140W	SPARS100	4	202.9
F153M	SPARS100	4	202.9
F164N	SPARS100	4	202.9
F167N	SPARS100	4	202.9
F160W	SPARS100	4	202.9
G102	SPARS100	4	202.9
G141	SPARS100	4	202.9

Table 1: IR01S08 exposures that were taken with a filter or grism in the optical path, listed in the order in which they were taken. Dark current ramps with the same sample sequence and number of reads were interleaved with the filtered ramps.

## **Analysis**

All ramps listed in Table 1 were first run through the IDL data reduction pipeline (Hilbert 2004), in order to remove bias signal and pixel-to-pixel variations in zero level, through subtraction of reference pixels and the zeroth read, respectively. Line-fitting up the 4-read ramps was used on a pixel-by-pixel basis, in order to calculate the measured signal rate. Finally, the signal rates for each ramp were multiplied by the TV3-measured

gain of  $2.26 \text{ e}^-/\text{ADU}$ . The end result was a single image for each ramp, giving the measured signal rate in units of electrons per second.

In each quadrant of each of the ramps, we created seven  $100 \times 100$  pixel boxes. A histogram of the signal rates within each box was fit with a Gaussian, and the peak value was recorded. We then took the median of these seven peak values in each quadrant, and recorded that value as the median measured background signal rate. The standard deviation of the seven peak values was recorded as the uncertainty in the background signal rate. Once the median and uncertainty had been calculated for each of the ramps, we were able to look for any trends in the measured background rates. Figure 1 shows the median background rates for all ramps except those obtained through the reddest filters, for reasons discussed below. Black points correspond to dark current ramps, while red points denote filtered ramps.

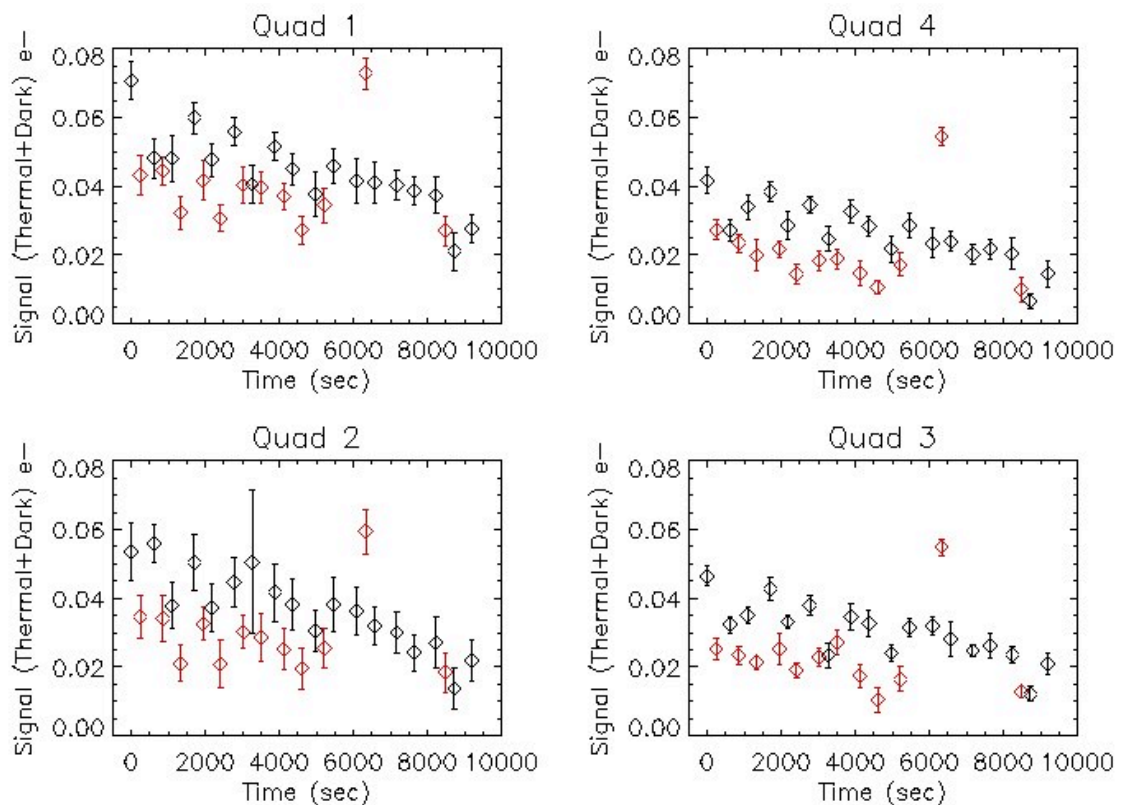


Figure 1: Median measured values of the dark current and background in the IR channel versus elapsed time of the test. Black points are signal rates in dark current files, while red points are those for filtered files, where each red point represents a different filter. Data were obtained moving from blue to red filters, so these plots can also be interpreted as being plotted versus increasing wavelength.

The first result to note is that the signal rate decreases with time. This trend was not seen in previous thermal vacuum testing (Robberto 2008), where the instrument set-up was identical to that in TV3, except for the detector. Observing logs indicate that 3 hours prior to the data for this background test being collected, the IR detector was exposed to

large flux levels during the non-linearity test. Early detector-level testing at the Detector Characterization Lab (DCL) indicate that persistence effects on this detector can be observed on a timescale of hours, depending on the illumination level. Figure 2 (DCL, private communication) shows the persistence effects on the flight detector after illuminating to 100 times the full well capacity. This plot shows that even 14 hours after illumination, the background level of the detector remained  $\sim 0.02$   $e^-/\text{sec}$  above the baseline rate. Relaxation times for lower illumination levels are shorter, although data do not exist for illuminations other than 100 times and half full-well. For the non-linearity test, the illumination was likely between 1 and 2 times full well. This implies that persistence effects are likely present in these background test data. As a result, calculated background values presented below should be viewed as upper limits.

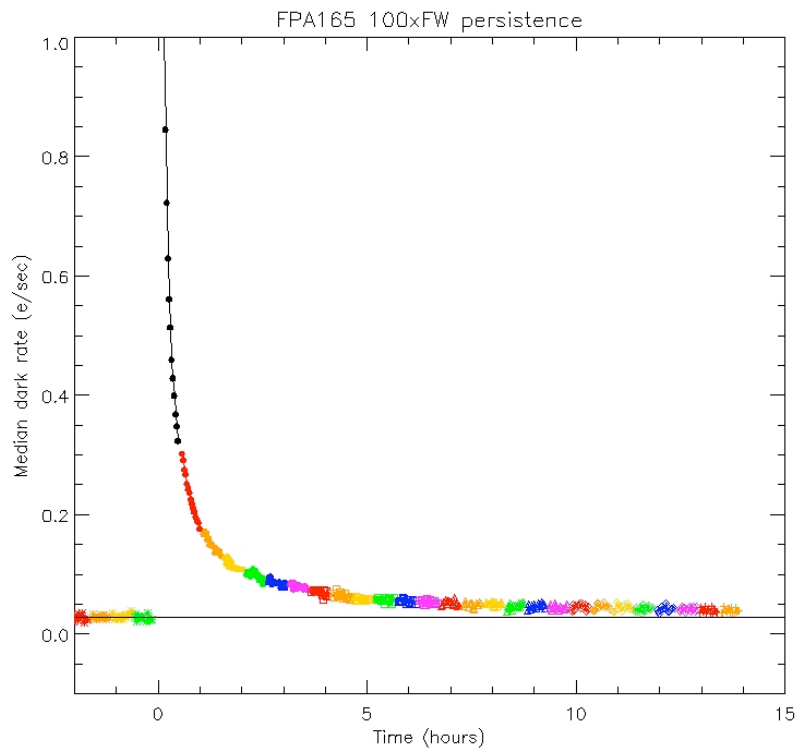


Figure 2: Background signal level measured at DCL, after illuminating the detector to signals of 100 times full-well.

Also seen in Figure 1, dark current ramps (black diamonds) show higher signal rates than neighboring filtered ramps (red diamonds). This behavior is consistent with that seen in TV2 testing. According to Roberto (2008), the difference in emissivity between the filters and the blank accounts for this difference in background signal rate. The blank is a piece of aluminum with a coating of de Soto black, while the filters are coated glass. The reflectivity of the filters is greater than that of the aluminum blank, leading to the

filters more effectively reflecting the blackbody radiation from the  $-85^{\circ}\text{C}$  radiation shield back onto the detector. This has the effect of making the filters appear colder than the aluminum blank, with less thermal emission.

Figure 3 is an expanded version of quadrant 1 in Figure 1, such that the measured background values from the reddest filters are visible. At wavelengths longer than about 1.4 microns, the thermal background contribution from the filter wheel and cold enclosure (at  $-44^{\circ}\text{C}$ ) quickly becomes the dominant source of signal. As seen in Figure 3, highly elevated background levels were observed through all filters with passbands extending longward of 1.4 microns. The F140W, F153M, F164N, F167N, and F160W filters, and G141 grism all show increased background signals, due to thermal emission of the instrument. The magnitudes of the background signal in these filters are equivalent to or less than those seen in TV2 (Robberto 2008). By calculating background rates separately for each quadrant, we show that while quadrants 1 and 2 show similar signals to those seen in TV2, quadrants 3 and 4 measure consistently lower background signals. This is true for data collected through all filters.

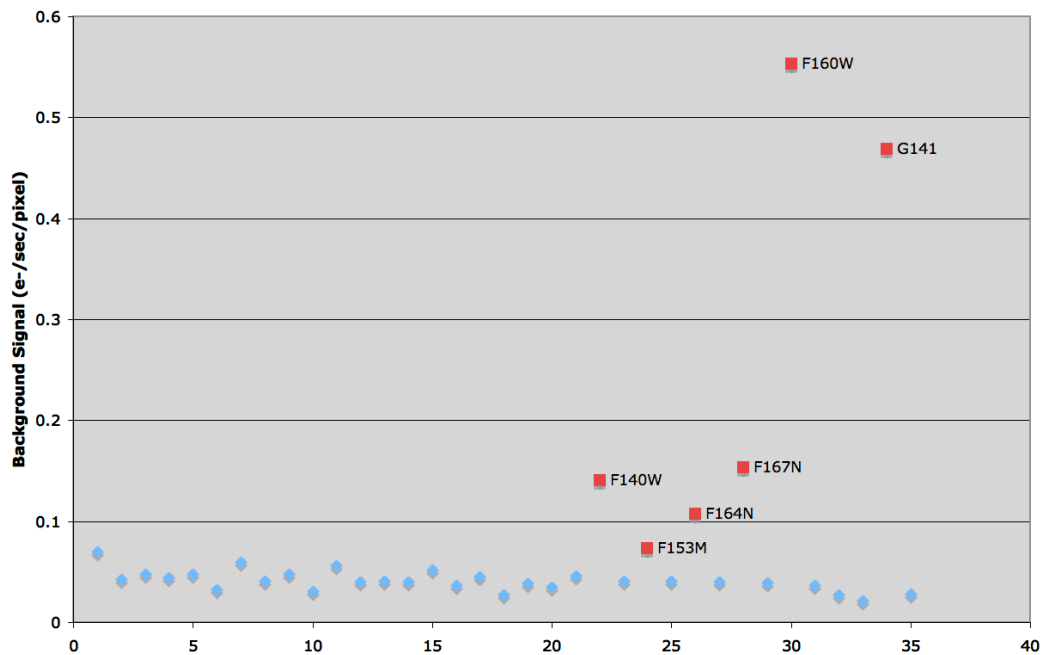


Figure 3: Expanded view of quadrant 1 in Figure 1. Filters where the thermal emission signal dominates are marked in red.

Table 2 gives tabulated results for the background signal rates and variations. The magnitudes and variations in Table 2 should be regarded as upper limits, due to the persistence effects from the non-linearity test performed prior to this one.

Filter	Median Background Signal Rate (e-) and Variation of Median During Test							
	Quad 1		Quad 2		Quad 3		Quad 4	
F098M	0.043	1.4%	0.034	1.5%	0.025	0.8%	0.027	0.7%
F105W	0.044	1.1%	0.034	1.7%	0.023	0.6%	0.023	0.6%
F110W	0.032	1.2%	0.021	1.3%	0.021	0.4%	0.020	1.2%
F125W	0.041	1.3%	0.032	1.2%	0.025	1.1%	0.022	0.6%
F126N	0.031	1.0%	0.021	1.8%	0.019	0.6%	0.014	0.7%
F127M	0.040	1.3%	0.030	1.2%	0.023	0.7%	0.018	0.7%
F128N	0.040	1.2%	0.028	1.7%	0.027	0.9%	0.019	0.7%
F130N	0.037	1.0%	0.025	1.5%	0.017	0.8%	0.015	0.9%
F132N	0.027	1.0%	0.020	1.5%	0.010	0.9%	0.011	0.5%
F139M	0.035	1.3%	0.025	1.4%	0.016	0.8%	0.017	0.9%
F140W	0.141	1.4%	0.125	2.2%	0.122	0.6%	0.124	0.6%
F153M	0.073	1.0%	0.059	1.6%	0.055	0.6%	0.054	0.7%
F164N	0.107	0.8%	0.096	3.8%	0.092	0.5%	0.091	0.7%
F167N	0.153	1.1%	0.137	1.4%	0.132	1.0%	0.134	0.3%
F160W	0.553	1.4%	0.514	3.9%	0.511	2.6%	0.530	1.3%
G102	0.027	1.1%	0.018	1.4%	0.013	0.5%	0.010	0.9%
G141	0.469	2.3%	0.439	3.3%	0.423	1.1%	0.436	2.2%

Table 2: Median measured background rates and variations in each quadrant for each filter. Variations are presented as percentages of the CEI Spec value of 0.4 e<sup>-</sup>/sec/pixel. Therefore, a variation greater than 10% would represent a failure to meet CEI Specification 4.4.8.2 (stability).

The CEI Specifications against which we are comparing our results cover both the magnitude and stability of the background signal in WFC3. CEI Specification 4.4.8.1 dictates that total background signal in the IR channel must be less than 0.4 e<sup>-</sup>/sec/pixel, with a goal of 0.1 e<sup>-</sup>/sec/pixel. In addition, CEI Specification 4.4.8.2 states that this background rate must be stable to 10% of the 0.4 e<sup>-</sup>/sec/pixel rate. Similarly, CEI Specification 4.8.4 says dark current plus internal background must be less than 0.4 e<sup>-</sup>/sec/pixel and calibratable to 10% over a period of 30 days. Our data only cover a period of 2.5 hours, so we cannot fully characterize the long-term stability of the background signal. But over the course of 2.5 hours, we already see variations greater than 10%. Absolute background signal levels easily meet the 0.4 e<sup>-</sup>/sec/pixel spec in all cases except the F160W filter and G141 grism. However, as detailed in the TV2 background analysis (Robberto 2008), the thermal background in the thermal vacuum chamber is larger than that expected on orbit, implying that the background in these two filters will fall below

0.4 e<sup>-</sup>/sec/pixel once WFC3 is installed into the Hubble. Roberto's model predicts that with the flight detector, the measured thermal background through the F160W filter and G141 grism will be 0.075 e<sup>-</sup>/sec/pixel and 0.070 e<sup>-</sup>/sec/pixel, both of which are well below the 0.4 e<sup>-</sup>/sec/pixel limit. The background signal should also be reduced once the effects of persistence are removed.

## **Recommendations**

Careful analysis of dark current data taken after high signal data from TV3 should be performed, in order to characterize the persistence behavior in the IR channel.

## **References**

Hilbert, B., 2004, WFC3 ISR 2004-10, "Basic IDL Data Reduction Algorithm for WFC3 IR and UVIS Channel"

Roberto, M., 2008, WFC3 ISR 2008-20, "Thermal Vacuum 2: measures of the IR background and on-orbit predictions (SMS IR01S18)"